Guanidine Hydrochloride-Induced Denaturation and Refolding of Transthyretin Exhibits a Marked Hysteresis: Equilibria with High Kinetic Barriers†

Zhihong Lai, Jennifer McCulloch, Hilal A. Lashuel, and Jeffery W. Kelly*

Department of Chemistry, Texas A&M University, College Station, Texas 77843-3255

Received December 30, 1996; Revised Manuscript Received April 14, 1997⊗

ABSTRACT: Fluorescence and circular dichroism spectroscopy as well as analytical ultracentrifugation and glutaraldehyde cross-linking were utilized to evaluate the tertiary and quaternary structural changes occurring on the denaturation and reconstitution pathways of transthyretin (TTR) as a function of guanidine hydrochloride (GdnHCl) concentration. These results demonstrate that the GdnHCl-mediated denaturation and reconstitution of TTR is reversible. However, the lowest GdnHCl concentration that dissociates and unfolds transthyretin does not allow the unfolded monomer to refold to tetramer at a rate that is measurable. As a result, there is a striking hysteresis observed upon comparison of the GdnHCl-mediated denaturation and reconstitution transitions. The TTR tetramer does not dissociate into unfolded monomer until the denaturant concentration exceeds 4 M GdnHCl, whereas unfolded monomeric TTR (denatured in 7 M GdnHCl) does not refold and assemble into a native tetrameric structure until the GdnHCl concentration is reduced to less than 2 M. These results imply that a significant kinetic barrier intervenes between the folded tetramer and unfolded monomer in both the denaturation and reconstitution directions at pH 7. A kinetics study of the denaturation of TTR as a function of GdnHCl concentration yields a first-order rate constant for unfolding of $(9.0 \pm 7.5) \times 10^{-11}$ s^{-1}, estimated by extrapolation of the rate constants for the tetramer to unfolded monomer transition as a function of GdnHCl to 0 M GdnHCl. This rate is very slow; as a result, wild-type TTR is predicted to be kinetically stable as a tetrameric quaternary structure once formed. These results imply that the rate of TTR dissociation and partial unfolding to the monomeric amyloidogenic intermediate under denaturing conditions may play a role in transthyretin-based amyloid diseases.

Transthyretin (TTR)[1] is a tetrameric human plasma protein that binds to both thyroxine and the retinol binding protein. The concentration of transthyretin is about 0.2 mg/mL; 3.63 $\mu M_{(tetramer)}$ in plasma and 0.017 mg/mL in cerebral spinal fluid. Transthyretin is composed of four identical subunits, each having a β-sandwich fold (Figure 1). The monomers dimerize through an intermolecular antiparallel β-sheet interaction between the H-strands and the resulting dimers associate in a face to face fashion, mainly through hydrophobic loop interactions affording a stable tetramer with an hourglass-shaped central channel where two molecules of thyroxine (T4) can bind (Blake et al., 1974, 1978; Hamilton et al., 1993). In unfortunate individuals, transthyretin is converted into an insoluble fibrilar structure referred to as amyloid (Benson, 1989; Benson & Wallace, 1989; Furuya et al., 1991; Jacobson & Buxbaum, 1991). These fibrils putatively cause senile systemic amyloidosis, when the fibrils are composed of wild-type TTR, and familial amyloid polyneuropathy, when one of 50 single-site TTR mutants is transformed into fibrils (Saraiva et al., 1983, 1984, 1988; Jacobson & Buxbaum, 1991; Cornwell et al., 1988; Westermark et al., 1990; Benson, 1989; Stone, 1990; Saraiva, 1995; Sipe, 1992, 1994). The age of onset of the senile disease is generally >80 years of age, whereas the age of onset for the familial form varies by mutation and is typically much earlier. The observed pathology appears to result from the amyloid's neurotoxicity and/or by the mass of fibrils physically interfering with normal organ function. A transthyretin amyloid fibril is approximately 130 Å in diameter and made up of four protofilaments, each having a twisted

FIGURE 1: Ribbon diagram of the TTR dimer explicitly showing the indole side chains of the tryptophan residues. The AB loops projecting from the back face in this view facilitate interactions with another dimer, leading to tetrameric TTR having a central channel.

† We gratefully acknowledge financial support of the National Institute of Health (R29 DK46335-01) and Tom Laue for helpful ultracentrifuge discussions.

* To whom correspondence should be addressed.

⊗ Abstract published in *Advance ACS Abstracts,* June 15, 1997.

[1] Abbreviations: TTR, transthyretin; FAP, familial amyloid polyneuropathy; SSA, senile systemic amyloidosis; GdnHCl, guanidine hydrochloride; SDS−PAGE, sodium dodecyl sulfate−polyacrylamide gel electrophoresis; CD, circular dichroism; *s*, sedimentation coefficient; S, Svedberg unit of 10^{-13} s; *D*, diffusion coefficient; dd, doubly distilled.

S0006-2960(96)03195-9 CCC: $14.00

cross-β sandwich structure (Blake & Serpell, 1996). Even though it is quite clear that conformational changes are required for human amyloid disease, it is not yet known how and where these conformational changes occur *in vivo* (Kelly, 1996). Lysosomal involvement in amyloid fibril formation is one possibility, which is supported by the lysosomal enzymes found to be associated with the amyloid fibrils in the extracellular space (Glenner et al., 1971; Cohen et al., 1983).

Following up on this possibility, we have shown that transthyretin (TTR) amyloid fibril formation is observed *in vitro* during partial acid denaturation (pH 5−4) and results from the self-association of a partially denatured intermediate of TTR (Colon & Kelly, 1991, 1992; Lai et al., 1996; Gustavsson et al., 1991). Transthyretin amyloid fibril formation can be avoided around pH 5 by working at low TTR concentrations and/or low temperatures, allowing identification of the quaternary, tertiary, and secondary structure of the intermediate(s) that lead to amyloid formation (Lai et al., 1996; Miroy et al., 1996). These studies reveal that tetrameric TTR is nonamyloidogenic. However, dissociation of the tetramer into a monomeric intermediate that undergoes an additional tertiary structural rearrangement affords the building block that is ultimately transformed into amyloid fibrils (Colon & Kelly, 1992; Lai et al., 1996). The familial amyloid polyneuropathy- (FAP-) associated TTR single-site variants studied thus far adopt a normal three-dimensional structure under physiological conditions based on crystallographic analysis; however, previous studies by our laboratory reveal that these mutations significantly destabilize the tetramer toward acid denaturation (McCutchen et al., 1993, 1995; Steinrauf et al., 1993; Hamilton et al., 1993; Terry et al., 1993). The mutation-induced destabilization allows the monomeric amyloidogenic intermediate to be populated under denaturing (lysosomal) conditions (pH 5.5 in the case of the FAP-associated Val-30-Met and the Leu-55-Pro TTR variants) where the wild-type protein remains predominantly tetrameric and nonamyloidogenic (McCutchen et al., 1993, 1995).

Partial denaturation appears to play a critical role in amyloid fibril formation in other human amyloid diseases as well, which has motivated us to look more carefully at the kinetics and thermodynamics of the denaturation and reconstitution pathways of transthyretin to gain further insight into amyloid fibril formation *in vivo* (Kelly, 1996; Hurle et al., 1994; Pepys et al., 1993; Come & Lansbury, 1994; Thomas et al., 1995; Lee et al., 1995; Fraser et al., 1994; Caughey et al., 1991; Prusiner, 1991). Acid denaturation, while likely relevant to fibril formation *in vivo*, does not allow quantitative measurements to be made regarding the thermodynamic stability of TTR. This capability is especially important to evaluate the stability of wild-type TTR relative to the FAP mutants, which are less stable toward acid denaturation (McCutchen et al., 1993, 1995). Therefore, the denaturation of TTR in chaotropic agents was examined in an attempt to extract this data. The most widely used chaotropic agents are GdnHCl and urea, both of which lower protein stability in proportion to their concentration (Dill & Shortle, 1991; Pace, 1975; Shortle et al., 1989). Denaturants such as urea or GdnHCl are thought to interact preferentially with the hydrophobic groups in the denatured state; however, the binding is very weak, which may explain the high concentrations required (Dill & Shortle, 1991).

A 1972 study of the chaotropic denaturation of TTR concludes that TTR does not dissociate into subunits in concentrations of urea as high as 8 M or in 6 M GdnHCl (Branch et al., 1972). Therefore, Branch and co-workers concluded that TTR was one of the most stable proteins examined up to that time. In the current study, fluorescence spectroscopy, circular dichroism, glutaraldehyde cross-linking, and analytical ultracentrifugation were used to characterize the denaturation and reconstitution pathway of TTR as a function of GdnHCl concentration, significantly extending and correcting Branch's earlier interpretations. An interesting aspect of the results of this study is the marked hysteresis observed during the unfolding and reconstitution of TTR. The TTR tetramer does not dissociate into monomer until the GdnHCl concentration exceeds 4 M, whereas unfolded and dissociated TTR (7 M GdnHCl) does not refold and assemble until the denaturant concentration is <2 M GdnHCl. These results imply that a significant kinetic barrier exists between the tetramer and the unfolded monomer at pH 7. This hypothesis is substantiated by a kinetic study of the denaturation of wild-type TTR at various GdnHCl concentrations. A first-order rate constant of $(9.0 \pm 7.5) \times 10^{-11}$ s^{-1} was obtained after extrapolation of the rate constants as a function of GdnHCl concentration to 0 M GdnHCl. This rate implies that wild-type TTR is kinetically stable in a tetrameric quaternary structure which should not dissociate on a biological time scale at pH 7, provided that the dissociation mechanism is the same in the presence and absence of GdnHCl.

MATERIALS AND METHODS

TTR was isolated and purified from recombinant sources as described previously (Lai et al., 1996). Ultrapure GdnHCl was obtained from ICN Biomedical. The silver stain kit used to visualize the PAGE gels was purchased from Sigma. All other reagents used were of highest quality available from Sigma or U.S.Biochemical Corp.

Fluorescence Emission Spectra in the Presence of Guanidine Hydrochloride. Fluorescence emission spectra of wt TTR were recorded on an SLM 8100 fluorometer at 20 °C in a 1 cm path length quartz cell using the photon counting method. Both of the excitation slits were set at 2 nm, while the emission slits were set at 4 nm. Excitation was accomplished at 295 nm, whereas the tryptophan emission spectra were collected from 300 to 430 nm. For denaturation studies, 0.01 mg/mL TTR solutions were prepared by diluting 20 μL of a 1.0 mg/mL TTR stock (in 10 mM phosphate, 100 mM KCl, and 1 mM EDTA, pH 7.4) into 1.98 mL GdnHCl solutions. The GdnHCl stock solution in 50 mM phosphate and 100 mM KCl buffer, pH 7 (the standard phosphate buffer), was made up as described by Pace et al. (1989), the final GdnHCl concentration being determined by refractive index. A 1.0 mg/mL TTR solution denatured in 7 M GdnHCl solution overnight was used to study reconstitution. Aliquots (20 μL) of denatured TTR were added to borosilicate glass culture tubes (from Fisher) containing the standard phosphate buffer (pH 7) and variable concentrations of GdnHCl. Each sample was mixed by vortexing and incubated for a minimum of 18 h at 20 °C before being evaluated. Samples incubated for periods up to 336 h were compared to the 18 h samples.

Far-UV CD-Monitored Denaturation and Reconstitution of TTR as a Function of GdnHCl Concentration. Circular

dichroism spectra were measured on an Aviv Model 62DS spectrometer at 20 °C, using a bandwidth of 1 nm and a time constant of 4 s. Signals at 218 nm were averaged 10 times for each sample. For denaturation and reconstitution studies, TTR at either 0.01 or 0.02 mg/mL was studied as a function of GdnHCl concentration in a 0.5 cm quartz cell using the standard phosphate buffer.

TTR Quaternary Structure Evaluated by Glutaraldehyde Cross-Linking. One hundred microliters of a 0.02 mg/mL TTR solution at a given GdnHCl concentration was prepared and incubated following the procedure described in sample preparation section for fluorescence. Two microliters of a 25% (w/v) glutaraldehyde solution was then added to each sample and the cross-linking reaction was allowed to proceed for 2 min. The cross-linking reaction was terminated by the addition of 2 μL of a 7% $NaBH_4$ solution dissolved in 0.1 M NaOH. Nine hundred microliters of dd H_2O was added to the cross-linking reaction after 15 min to dilute the GdnHCl, which facilitated TTR precipitation, accomplished by adding 8 μL of 25% deoxycholic acid solution and 25 μL of 78% trichloroacetic acid. The samples were centrifuged at 14 000 rpm for 10 min, and the solution was removed by suction. The pellet was then resuspended in 30 μL of 5% SDS sample buffer and incubated in a boiling water bath for 10 min. These samples were then loaded onto a 12% SDS−polyacrylamide gel, which was developed with the silver stain kit from Sigma.

Probing TTR Quaternary Structure by Analytical Ultracentrifugation. TTR solutions (0.02 mg/mL) undergoing denaturation or reconstitution as a function of GdnHCl concentration were made up following the procedures described in the fluorescence section above. Sedimentation velocity and equilibrium data were collected on a temperature-controlled Beckman XL-A analytical ultracentrifuge equipped with a An60Ti rotor and photoelectric scanner. For sedimentation velocity runs, a double sector cell equipped with a 12 mm Epon centerpiece and quartz windows was loaded with 400−420 μL of solution using a blunt-end microsyringe. Data were collected in a continuous mode at 20 °C, employing a step size of 0.005 cm, an average of 4 scans/point, and rotor speeds of 3000−60 000 rpm. The Svedberg program developed by Philo (1994) was used to directly fit the sedimentation concentration profiles, from which the sedimentation coefficient (*s*) and the diffusion coefficient (*D*) could be determined. The observed sedimentation coefficient, *s*, was corrected to standard conditions with the following equation using tabulated density and viscosity:

$$s_{20,w} = s\frac{(\eta)_{T,\beta}}{(\eta)_{20,\omega}}\frac{(1-\bar{v}\rho)_{20,\omega}}{(1-\bar{v}\rho)_{T,\beta}} \quad (1)$$

where ρ and η are the density and viscosity of water at 20 °C, respectively, and $\bar{v}$ is the partial specific volume of TTR. The density and viscosity were calculated using polynomial equations and tables of coefficients (Laue, 1992). The partial specific volume of TTR (0.735 cm^3/g) was estimated on the basis of the partial specific volumes of the component amino acid residues (see below for more info on $\bar{v}$) (Durchschlag, 1986; McMeekin & Marshall, 1952; Perkins, 1986; Durchschlag & Jaenicke, 1982).

Sedimentation equilibrium runs were performed on 110 μL samples from 3000−20 000 rpm using six-sector cells with charcoal-filled Epon centerpieces and sapphire windows. All scans were performed at 220 nm, with a step size of 0.001 and 50 averages/point. Samples were allowed to equilibrate in the centrifugal field for 72−80 h, and duplicate scans 3 h apart were overlaid to determine that equilibrium had been reached. The data were analyzed by a nonlinear least-squares analysis using the Origin software provided by Beckman. The data were fit to a single ideal species model using the following equation to determine the best-fitting molecular weight,

$$A_r = \exp[\ln(A_0) + (M\omega^2(1-\bar{v}\rho)/2RT)(x^2 - x_0^2)] + E \quad (2)$$

where A_r is the absorbance at radius x, A_0 is the absorbance at a reference radius x_0 (usually the meniscus), $\bar{v}$ is the partial specific volume of TTR (milliliters per gram), ρ is the density of the solvent (grams per milliliter), ω is the angular velocity of the rotor (radians per second), E is the baseline error correction factor, M is the molecular weight, R is the universal gas constant, 8.314×10^7 erg/mol, and T is temperature (kelvin). The approximations of $\bar{v}$ based on amino acid composition are typically in error by less than 1%, which corresponds to a 3% error in MW (Perkins, 1986; Durchschlag, 1986). The error in $\bar{v}$ can be as large as 3% for nonglobular structures affording a maximum error in MW of 9%. The partial specific volume is corrected for temperature effects $\bar{v}_T = \bar{v}_{25\,°C} + (4.25 \times 10^{-4})(T - 25)$ (Laue et al., 1992). The partial specific volume is also corrected for added GdnHCl yielding an apparent isopotential partial specific volume of the protein in GdnHCl ($\phi_{[GdnHCl]}$) using the following equation: $\phi_{[GdnHCl]} = \bar{v} - (1/\rho - \bar{v}_3)(A_3 - g_3A_1)$ where $\bar{v}_3$ is the partial specific volume of GdnHCl, A_3 is the absolute solvation, i.e., grams of denaturant bound per gram of protein, A_1 is the total hydration, and g_3 is the solvent composition, expressed as gram of denaturant per gram of H_2O (only valid for 6 M GdnHCl) (Lee & Timasheff, 1979). Experimentally, the partial specific volume of a protein at intermediary GdnHCl concentrations varies in a nonlinear fashion, but typically not by more than 0.03 (4%), leading to a maximal error in MW of ≈12% (Durchschlag & Jaenicke, 1982).

Determination of the First-Order Rate Constant for TTR Tetramer Dissociation to Monomer by Far-UV CD. Denaturation kinetics were measured on an Aviv Model 62DS spectrometer at 20 °C. Twenty microliters of 1.0 mg/mL TTR stock was added to 980 μL of GdnHCl solution in the standard phosphate buffer preincubated at 20 °C in a 0.5 cm path length quartz cell. The sample was vortexed briefly, and the change in the CD signal upon denaturation was followed at 218 nm. (At 215 nm, which is the minimum of the far-UV CD spectrum of native TTR, the noise level was too high at 7 M GdnHCl due to the 0.5 cm path length cell used.) The manual mixing process took 20 s on average. After the kinetic data for denaturation were collected, the GdnHCl concentration of each solution was determined by refractive index. The first-order rate constant for TTR denaturation was evaluated at a number of different GdnHCl concentrations. The change of signal could be fit to the equation $Y = Y_A[A] + Y_B([A_0] - [A])$, with Y = CD signal, Y_A = CD signal of tetramer, Y_B = CD signal of unfolded monomer, $[A_0]$ = initial tetramer concentration, and $[A]$ = the concentration of tetramer determined by the first-order rate equation $[A] = [A]_0\, e^{-kt}$, where k = first-order rate constant and t = time in seconds. The Kaleidagraph program

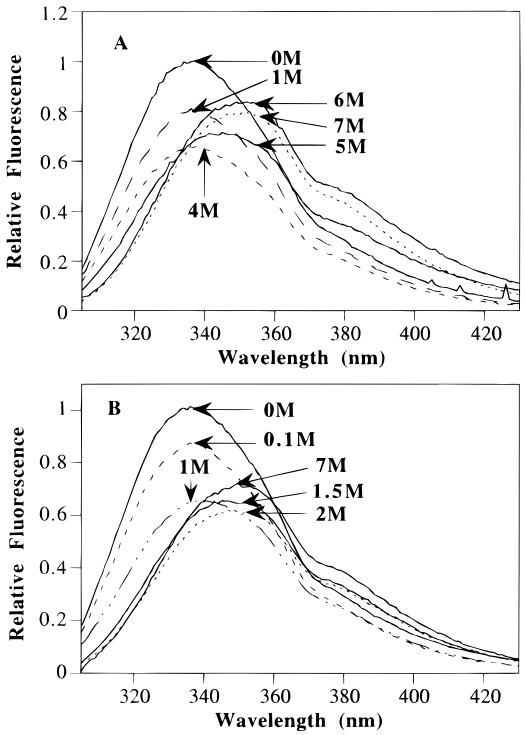

FIGURE 2: Tryptophan emission spectra of TTR (0.01 mg/mL) as a function of GdnHCl (excitation at 295 nm). (A) Denaturation-induced fluorescence changes as a function of added GdnHCl. (B) Reconstitution-induced fluorescence changes as a function of [GdnHCl].

(Synergy Software, Reading, PA) was used to fit the data to the above equation.

RESULTS

Denaturation and Reconstitution of TTR Monitored by Fluorescence. Fluorescence intensity has been widely used to characterize protein structural changes in chaotropic solutions and is usually directly related to the population of macrostates for an N ↔ U transition. The wavelength of maximum fluorescence emission (λ_{max}) as a function of GdnHCl, however, can give a skewed tracking of the population of states but is very useful for characterizing the environment of the indole side chain(s) as a function of denaturant concentration (Eftink, 1994). The tryptophan emission spectral changes associated with the denaturation of TTR are shown in Figure 2A. Native TTR has a fluorescence maximum at about 335 nm that decreases in intensity and red-shifts to approximately 350 nm upon treatment with 7 M GdnHCl. At intermediate GdnHCl concentrations, the denaturation behavior of TTR monitored by fluorescence is complex. From 0 to 4 M GdnHCl, the fluorescence intensity decreases by about 30% but the emission maximum does not significantly red-shift. Over the GdnHCl range of 4−6 M, the fluorescence intensity increases by 15% and the spectral maximum red-shifts significantly to 350 nm, consistent with the exposure of the tryptophans to denaturant. In the concentration range of 6−7 M GdnHCl, both the intensity and wavelength of indole emission remain nearly constant. The emission spectra characteristic of TTR undergoing reconstitution at various GdnHCl concentrations are shown in Figure 2B. Samples incubated in 7 M GdnHCl and diluted to 2 M GdnHCl exhibit similar fluorescence spectra. In fact, the intensity and emission maximum of tryptophan fluorescence remain nearly

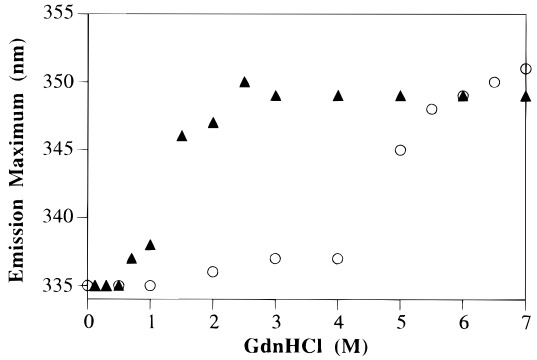

FIGURE 3: Emission wavelength of maximum tryptophan fluorescence as a function of GdnHCl concentration. Denaturation of TTR is represented by circles, and reconstitution of TTR indicated by triangles.

constant over the denaturant range of 7−2 M GdnHCl. The major blue shift in the fluorescence emission spectrum occurred upon dilution to a final GdnHCl concentration between 1 and 2 M. Reconstituted TTR at 0.1 M GdnHCl has the same emission wavelength as the native protein (0 M GdnHCl), although the intensity is 10% lower. It is unclear what causes the lowered fluorescence intensity; however, the protein appears to be properly folded owing to its native T4 binding and its native far-UV CD spectrum. However, we cannot rule out a subtle conformational difference between the recombinant folded and GdnHCl-reconstituted TTR. Comparing the denaturation and reconstitution of TTR, it is clear that the major denaturation event occurs at 4−6 M GdnHCl, while the reconstitution occurs between 1 and 2 M GdnHCl. The emission maximum wavelength of TTR as a function of GdnHCl concentration is plotted in Figure 3, to show the hysteresis of the unfolding and refolding transition, rather than to track the population of the different states accurately, as there are likely to be several intermediate states involved. From this figure, it can be discerned that the unfolding of TTR by GdnHCl is not a thermodynamically reversible process at a given GdnHCl concentration either in the denaturation or reconstitution transition region (Pace et al., 1989). Incubation of the samples for up to 336 h yields identical fluorescence data, implying that we are not simply dealing with slow equilibria.

Far-UV CD-Monitored TTR Denaturation and Reconstitution in GdnHCl. To understand the changes in the β-sheet tertiary structure exhibited by TTR as it unfolds and refolds in GdnHCl, far-UV CD spectra of TTR (0.02 mg/mL) were recorded. The circular dichroism spectrum of native TTR, exhibiting a 215 nm minimum in the far UV region (Figure 4A), is consistent with the predominantly β-sheet structure determined by X-ray crystallography (Blake et al., 1974, 1978; Lai et al., 1996). Upon treatment of TTR with 7 M GdnHCl, the far-UV CD spectrum shows a large decrease in intensity at 218 nm due to loss of the β-sheet tertiary structure (Figure 4A). The tryptophan fluorescence maximum (350 nm, Figure 2A) and far-UV CD spectral data indicate that TTR is largely unfolded in the presence of 7 M GdnHCl. When TTR was refolded in 0.1 M GdnHCl by dilution of denatured TTR (7 M GdnHCl), the far-UV CD spectrum shows nativelike signal, indicating reconstitution of TTR into a β-sheet structure (Figure 4A). In addition, the emission maximum of the tryptophans (335 nm) indicates that they are partially buried, as in the native structure (Figure 2B). The circular dichroism signal at 218 nm, reporting on β-sheet content, was chosen to study the denaturation and

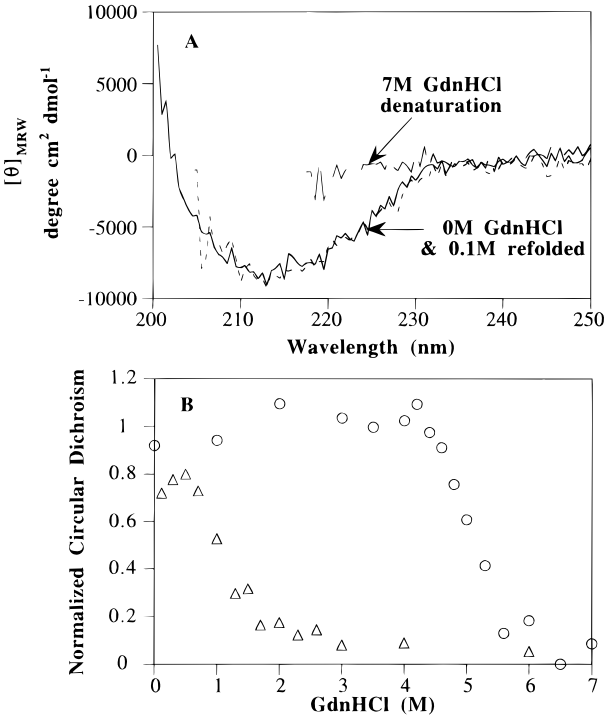

FIGURE 4: Transthyretin far-UV CD data resulting from denaturation and reconstitution as a function of GdnHCl concentration. (A) Far-UV CD spectra of TTR recorded in 0 and 7 M GdnHCl and a spectrum recorded after TTR reconstitution facilitated by diluting denatured TTR (7 M GdnHCl) to 0.1 M GdnHCl. (B) Far-UV CD intensity at 218 nm employed to monitor denaturation (circles) and reconstitution (triangles) of TTR (0.01 mg/mL) as a function of GdnHCl concentration.

reconstitution of TTR (0.02 mg/mL) to confirm the hysteresis observed by fluorescence. The denaturation and reconstitution transitions monitored by far-UV CD shown in Figure 4B are very similar to the transitions exhibited by fluorescence. The denaturation and reconstitution processes monitored by far-UV CD were also studied at a TTR concentration of 0.01 mg/mL to allow a direct comparison with the fluorescence study carried out at the same concentration. From the denaturation curve, it seems that TTR retains most of its β-sheet structure up to 4 M GdnHCl. The major unfolding transition occurs between 4 and 6 M GdnHCl, and above 6 M GdnHCl the CD signal remains constant consistent with an unstructured polypeptide chain. For the reconstitution transition, the CD signals are consistent with a random coil structure over a GdnHCl concentration of 7−2 M (Figure 4B). Over the GdnHCl concentration range of 2−0.1 M, the signal increases to 70−80% of the native signal intensity. Again, these results show that the denaturation and reconstitution transitions are separated by a significant GdnHCl concentration difference (Δ[GdnHCl] = 4 M), verifying the hysteresis observed by fluorescence-monitored GdnHCl denaturation and reconstitution of TTR. An analogous CD evaluation carried out after a week of incubation demonstrated that the hysteresis persisted.

TTR Quaternary Structural Changes upon Denaturation and Reconstitution in GdnHCl by Glutaraldehyde Cross-Linking. A method utilizing glutaraldehyde to cross-link TTR in the presence of GdnHCl was used to study the quaternary structure of TTR as a function of denaturant concentration and to identify conditions suitable for further evaluation by ultracentrifugation analysis. The quaternary structure of TTR (0.02 mg/mL) as a function of GdnHCl

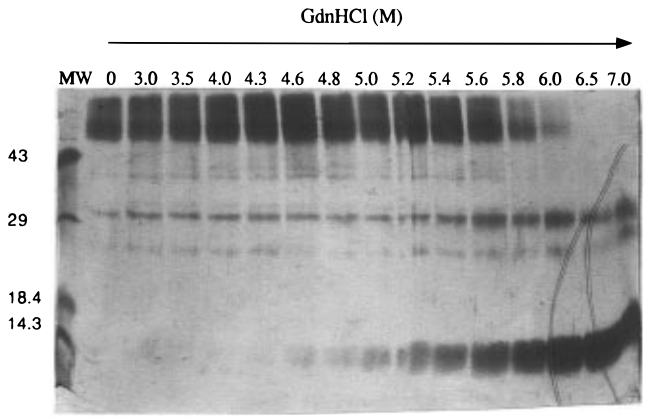

FIGURE 5: SDS−polyacrylamide gel showing the quaternary structure of TTR during denaturation as a function of GdnHCl concentration (after cross-linking with glutaraldehyde). Lane 1 displays labeled MW markers. TTR is predominantly tetrameric from 0 to 4.3 M GdnHCl as discerned by the band at 54 kDa. At GdnHCl concentrations > 4.6 M, TTR begins to dissociate to monomer (14 kDa); the dissociation is complete at 6.5 M GdnHCl.

(0−6 M) after a 24 h incubation is shown in the PAGE gel of cross-linked TTR in Figure 5. From 0 to 4.3 M GdnHCl, TTR exists as a tetramer as discerned by the tetrameric band around 54 kDa. This tetrameric band is only seen after cross-linking, as the normal TTR tetramer is SDS-sensitive (denatures to a dimer that is resistant to SDS). A transition from tetramer to monomer can clearly be seen over the GdnHCl concentration range of 4.6−6.0 M. Above 6 M GdnHCl, TTR is predominantly if not completely monomeric. The dimeric band observed in the gel (5−10%) appears to result from the [GdnHCl] dependence on the efficiency of the cross-linking reaction. Incomplete cross-linking of the tetramers at low GdnHCl and a small amount of intermolecular cross-linking of the TTR monomers at high GdnHCl concentrations best explain this band. This interpretation is consistent with the analytical equilibrium ultracentrifugation and sedimentation velocity data, which does not detect dimer in solution, implying that there is <7% dimer in solution (*vide infra*). A similar cross-linking analysis for the reconstitution of TTR (at a final TTR concentration of 0.02 mg/mL, sample initially denatured in 7 M GdnHCl) shows that TTR exists as monomer over the GdnHCl concentration range of 7−2 M. The monomer to tetramer quaternary structural transition occurs between 2 and 1 M GdnHCl. Below 1 M GdnHCl, the tetramer is the major TTR quaternary structure identified by this analysis. These results, when considered in the context of the tertiary structural changes discussed above, suggest that the tertiary and quaternary structural changes observed during denaturation and reconstitution are likely linked.

TTR Quaternary Structure in GdnHCl by Analytical Ultracentrifugation. Analytical ultracentrifugation was used to further evaluate the quaternary structure of TTR as a function of GdnHCl concentration. The sedimentation coefficients obtained from velocity analysis and apparent molecular weights obtained from equilibrium analysis of TTR undergoing denaturation and reconstitution in GdnHCl (0.02 mg/mL) are summarized in Table 1. For TTR exposed to denaturing conditions in 4 M GdnHCl, sedimentation velocity studies analyzed by the Svedberg program exhibit a fit to a single ideal species with $s_{20,w} = 4.3$ S (S is the abbreviation for Svedberg units, 10^{-13} s), indicating that TTR still exists in tetrameric form in 4 M GdnHCl. Upon exposure of TTR

Table 1: Sedimentation Coefficients and Molecular Weights of TTR (0.02 mg/mL) Undergoing Denaturation and Reconstitution in GdnHCl As Discerned by Analytical Ultracentrifugation Studies[a]

solution	sedimentation velocity		sedimentation equilibrium (Da)
	s (S)	$s_{20,w}$ (S)	
4.0 M (denaturation)	1.96	4.34	33435 ± 132
6.0 M (denaturation)			16103 ± 46
0.14 M (renaturation)	3.79	4.13	51997 ± 3442
2.0 M (renaturation)	0.96	1.43	13827 ± 390

[a] TTR tetramer MW = 54 980 and monomer MW = 13 745).

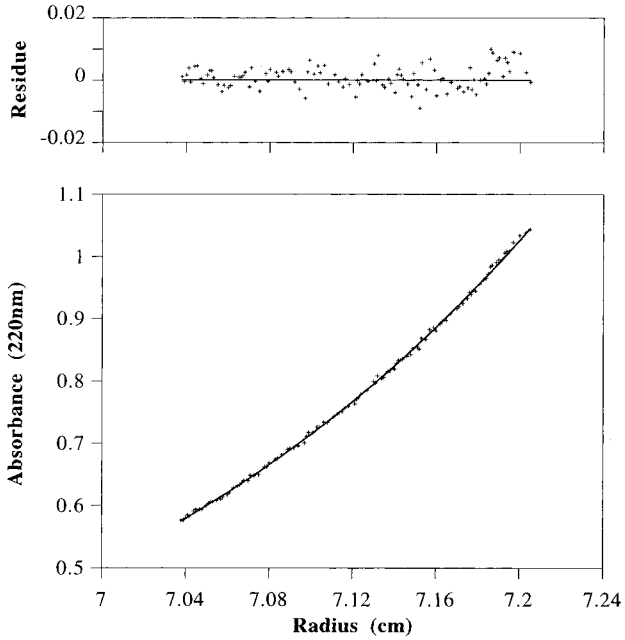

FIGURE 6: Sedimentation equilibrium analysis of TTR (0.02 mg/mL) denatured in 6 M GdnHCl. The solid line drawn through the data was obtained by fitting the absorbance vs radial position to eq 2 for a single ideal species. The residuals (difference between the experimental data and the fitted data for each point) are shown in the top panel.

to 5 and 6 M GdnHCl, good sedimentation velocity data was obtained; however, none of the methods used would fit the data well owing to transthyretin's small s value under these conditions. If TTR exists as denatured monomer as suggested by the cross-linking and spectroscopic data discussed above, it would sediment with an s value around 0.3 S due to the high density and viscosity of the concentrated GdnHCl solutions employed. This small s value exceeds the lower limit for Svedberg analysis and most of the existing methods of analysis. Therefore, sedimentation equilibrium experiments were used to characterize the quaternary structure of TTR in 6 M GdnHCl. The equilibrium data on TTR fits well (random residuals) to a single ideal species (Figure 6), having a MW of 13 929, in excellent agreement with monomeric TTR as the predominant species in 6 M GdnHCl. Equilibrium analysis of TTR denatured in 4 M GdnHCl yields an average molecular weight that is less than that expected for the tetramer but still significantly higher than monomer. This result may or may not be a consequence of the extended run times (72 h) required to reach equilibrium in 4 M GdnHCl; nevertheless, this result is not consistent with monomeric TTR.

For TTR undergoing reconstitution (7 M GdnHCl) by dilution to 2.0 and 0.14 M GdnHCl, the equilibrium analysis affords molecular weights corresponding to a monomer and tetramer, respectively (Table 1). The sedimentation velocity

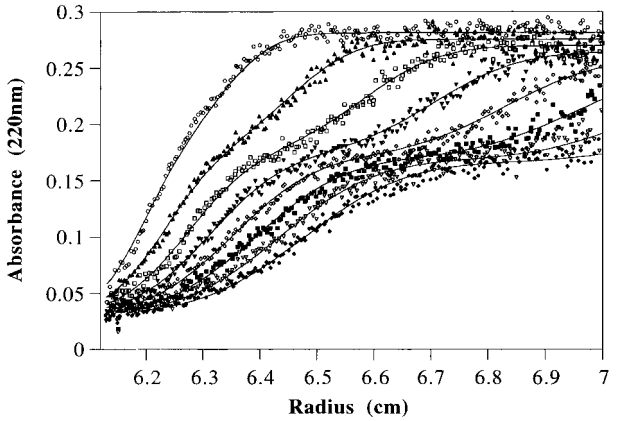

FIGURE 7: Sedimentation velocity profile of TTR (0.02 mg/mL) undergoing reconstitution by dilution into 1.0 M GdnHCl. The solid lines represent the two-species fit to the experimental data using the Svedberg program. The different symbols represent the experimental data sets collected at 15 min intervals as the sample sediments toward the bottom of the cell.

analysis reveals that TTR refolded by dilution to 2.0 M has a small s value of 0.96 S, which corresponds to $s_{20,w} = 1.4$ S. This s value agrees well with monomeric TTR and the s value previously obtained for monomeric TTR unfolded at pH 2 in the absence of salt ($s_{20,w} = 1.2$ S) (Lai et al., 1997). The sedimentation velocity analysis of TTR refolded by dilution to 0.14 M GdnHCl exhibits a sedimentation coefficient $s_{20,w}$ of 4.13 S, consistent with tetrameric TTR, as TTR sediments with $s_{20,w} = 4.2$ S under native conditions. Stafford's $g(s^*)$ analysis of the 0.14 M GdnHCl velocity data confirms the presence of a single species with s value approximately equal to 3.8 S, consistent with tetrameric TTR (data not shown) (Stafford, 1994). The sedimentation velocity analysis of TTR refolded by dilution to 1 M GdnHCl shows evidence for both monomer and tetramer as discerned by Svedberg analysis (Philo, 1994). Svedberg analysis works very well for evaluating s values smaller than 2 S, where diffusion dominates and the boundaries are very broad. The sedimentation velocity profiles of TTR reconstituted in 1.0 M GdnHCl shown in Figure 7 clearly have two well-separated boundaries. The Svedberg program fits the data to two noninteracting species, $s_1 = 1.26$ S and $s_2 = 3.396$ S, which corresponds to $s_{20,w,1} = 1.61$ S and $s_{20,w,2} = 4.30$ S (Philo, 1994). This data indicates that TTR exists as a mixture of tetramer and monomer under these conditions; however, these species do not appear to be in equilibrium. Svedberg analysis fits the initial absorbance of each species to $c_1 = 0.213$ and $c_2 = 0.095$, which corresponds to roughly 70% monomer and 30% tetramer in 1.0 M GdnHCl.

The above experiments demonstrate conclusively that the quaternary structural changes accompanying the unfolding of TTR in GdnHCl are not reversible at a fixed GdnHCl concentration in either the denaturation or reconstitution transitions. Furthermore, there is a strong hysteresis between the denaturation and reconstitution of TTR with regard to quaternary structural changes. For example, the TTR tetramer is stable at 2 M GdnHCl, but after being unfolded in 7 M GdnHCl, TTR remains monomeric and unfolded when the GdnHCl concentration is diluted to 2 M. The observed hysteresis suggests that the rate of interconversion between certain quaternary forms is very slow under certain conditions, so that equilibrium is not achieved on a practical time scale. This prevents direct measurement of the equilibrium constant and thus the conformational stability of the TTR

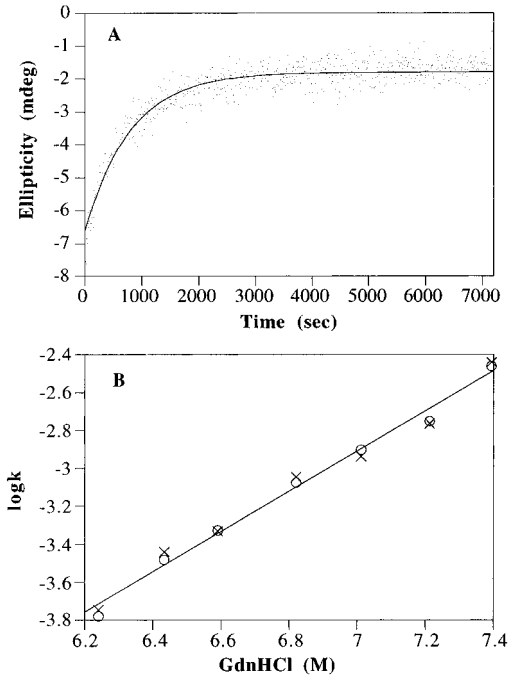

FIGURE 8: Determination of the first-order rate constant for denaturation of the TTR tetramer (0.02 mg/mL) to the unfolded monomer. (A) The disappearance of β-sheet signal at 218 nm is fitted by a single exponential at each GdnHCl concentration. The representative time course shown here is for denaturation at 7 M GdnHCl. (B) The observed first-order rate constants are plotted as a function of GdnHCl concentration for two representative trials, trial 1 (○) and trial 2 (×). Extrapolation of the rate constants to 0 M GdnHCl yields $k = (9.0 \pm 7.5) \times 10^{-11}$ s^{-1} for denaturation of TTR tetramer under native conditions.

tetramer. However, an estimate of the kinetic stability of the TTR tetramer was achieved by measuring the rate constant for denaturation of the TTR tetramer as a function of GdnHCl concentration.

Determination of the First-Order Rate Constant for TTR Tetramer Dissociation into an Unfolded Monomer. The rate of denaturation of the TTR tetramer to unfolded monomer was determined by monitoring the disappearance of β-sheet signal at 218 nm following dilution of TTR into a series of GdnHCl solutions at 20 °C (Figure 8A). Over the GdnHCl concentration range of 6.2−7.4 M, the denaturation time course was amenable to evaluation by manual mixing methods. Since the kinetic constants are very sensitive to the GdnHCl concentration, the GdnHCl concentration of each of the solutions was determined by refractive index after the kinetic data were collected. Each time course was fit to a single exponential to determine the rate constant for unfolding at a particular GdnHCl concentration. The rate constants determined are the microscopic rate constants of unfolding, since there is no contribution from the refolding reaction under the conditions of measurement. The rate constants as a function of GdnHCl were extrapolated to native conditions (no denaturant) to obtain an estimate of the first-order rate constant characterizing dissociation of TTR tetramer of $(9.0 \pm 7.5) \times 10^{-11}$ s^{-1} (Figure 8B), which corresponds to a half-life of about 293 years. This rate is so slow that once the TTR tetramer is formed, it does not dissociate on a biologically relevant time scale under nondenaturing conditions. This interpretation assumes that the rate-determining step does not change under physiological conditions.

DISCUSSION

The study of the denaturation and reconstitution of TTR by fluorescence, CD, glutaraldehyde cross-linking, and analytical ultracentrifugation demonstrates that there is a striking hysteresis between the GdnHCl denaturation and reconstitution curves. The changes in TTR quaternary and tertiary structures appear to be linked as the tetramer dissociates and unfolds between 4 and 6 M GdnHCl. Yet the denatured TTR (7 M GdnHCl) will not undergo reconstitution at 4 M GdnHCl. In fact, the GdnHCl concentration must be less than 2 M to observe reconstitution. These results demonstrate that the denaturation and reconstitution are kinetically determined.

Since the denaturation and reconstitution transitions are not reversible at a given GdnHCl concentration, we will consider them separately. The changes in TTR quaternary structure occurring during denaturation in GdnHCl were followed by glutaraldehyde cross-linking and analytical ultracentrifugation studies. The glutaraldehyde cross-linking method allows direct visualization of the quaternary forms of TTR on a silver-stained SDS−PAGE gel as a function of GdnHCl concentration. The cross-linking methodology demonstrates that varying proportions of TTR tetramer and monomer are the major species present during denaturation employing GdnHCl. Incomplete cross-linking of the tetramers at low GdnHCl concentration and a small amount of intermolecular cross-linking of the monomers at high GdnHCl concentrations best explain the dimer band representing ≤10% of total TTR. The transition from tetramer to monomer occurs between 4.6 and 6 M GdnHCl. Analytical ultracentrifugation (sedimentation velocity and sedimentation equilibrium) studies demonstrate conclusively that the tetramer to monomer transition is taking place over this concentration range.

Intrinsic tryptophan fluorescence was employed to follow the tertiary structural changes occurring within TTR during denaturation. From 0 to 4 M GdnHCl, the fluorescence intensity at 335 nm decreased by about 30% without a significant change in emission wavelength. The 30% decrease of fluorescence intensity observed up to 4 M GdnHCl may be caused by a tertiary structural rearrangement involving a tryptophan residue(s) in tetrameric TTR, or because of the increased mobility of the local environment of the tryptophans, or perhaps the solvent-dependent change in indole fluorescence is dramatic (a very steep baseline). A combination of these factors may also be responsible. From 4 to 6 M GdnHCl, the fluorescence intensity increases by 15% and the spectral maximum shifts to longer wavelength consistent with linked dissociation and unfolding. In the range of 6−7 M GdnHCl, both the intensity and wavelength maximum of emission remain constant, consistent with an ensemble of interconverting conformations. Above 6 M GdnHCl, no higher MW TTR quaternary structures were detected in the ultracentrifuge experiments; hence, at least 95% of TTR is in the monomeric form.

Fluorescence spectra of the single-tryptophan-containing variants (W41F and W79F) show that Trp-41 is the major contributor to the TTR fluorescence emission spectra observed under physiological conditions, while Trp-79 is completely quenched under native conditions in tetrameric TTR (Lai et al., 1996). Trp-41 is located in the loop proximal to the start of β-strand C, and Trp-79 is in the helix intervening between strands E and F (Figure 1). It is likely

that the decrease in fluorescence intensity observed from 0 to 4 M GdnHCl arises from the interaction between Trp-41 and the solvent. The increased mobility (exposure to solvent) is possibly coupled to a local rearrangement in the C-strand−loop−D-strand loop region, which was observed during acid denaturation and appears to be important in amyloid fibril formation (Miroy et al., unpublished results; Lai et al., 1996; Kelly & Lansbury, 1994; Blake & Serpell 1996). The increase in fluorescence intensity as well as the red-shifted emission to 350 nm from 4 to 6 M GdnHCl suggests global unfolding of TTR. The increase in fluorescence intensity observed at 350 nm is most likely due to the fluorescence of Trp-79, which is separated from its quencher upon unfolding. Ongoing studies of the fluorescence of the single-tryptophan-containing variants W41F and W79F as a function of GdnHCl suggest that the above explanation is likely to be correct (data not shown).

The denaturation of TTR evaluated by changes in the far-UV CD spectrum as a function of GdnHCl further support linked dissociation and unfolding. The CD signal remains fairly constant over the GdnHCl concentration of 0−4 M, suggesting that the β-sheet content of the tetrameric TTR does not change appreciably over this GdnHCl range. This data does not contradict the rearranged tetramer proposed previously as the β-sheet core still remains intact in the rearranged tetramer. Only the C-strand−loop−D-strand region appears to become more mobile, which probably does not contribute to the β-sheet minimum at 215 nm in the native fold due to its highly twisted nature. At GdnHCl concentrations ≥ 6 M, TTR is unfolded as discerned by the loss of the 218 nm minimum in the CD spectrum characteristic of sheet structure. Unfortunately, the CD minimum at 197 nm associated with an ensemble of interconverting conformations is not observable owing to the high absorbance of GdnHCl; however, the tryptophan fluorescence emission maximum at 350 nm in 6 M GdnHCl is consistent with that expected from an ensemble of interconverting conformations (Lakowicz, 1983). Linked dissociation and unfolding in 6 M GdnHCl is fully consistent with the monomeric nature of TTR supported by analytical ultracentrifugation results discussed above.

Unlike the denaturation transition, which occurs over a GdnHCl concentration range of 4−6 M, the reconstitution transition (folding and association) is observed at much lower GdnHCl concentrations. As discussed above, TTR adopts an unfolded monomeric conformation in 6−7 M GdnHCl. Upon dilution of this unfolded monomer to lower GdnHCl concentrations, glutaraldehyde cross-linking and ultracentrifugation analyses indicate that assembly from monomer to tetramer occurs only at concentrations below 2 M GdnHCl. Sedimentation equilibrium and velocity analysis agree that tetrameric TTR is the primary species observed when TTR is diluted from 7 M to 0.1 M GdnHCl. At 1 M GdnHCl, sedimentation velocity analysis clearly shows the separation of two boundaries corresponding to TTR tetramer and monomer, which do not appear to be in equilibrium, while at 2 M GdnHCl, the molecular weight obtained from sedimentation equilibrium is consistent with TTR monomer.

The fluorescence-monitored reconstitution (linked folding and association) of TTR exhibits a 15 nm blue shift as unfolded TTR (7 M) is diluted to GdnHCl concentrations below 1 M, consistent with the partial burial of the tryptophan residues in a nativelike tertiary structure. The β-sheet content monitored by far-UV CD at 218 nm also shows a transition

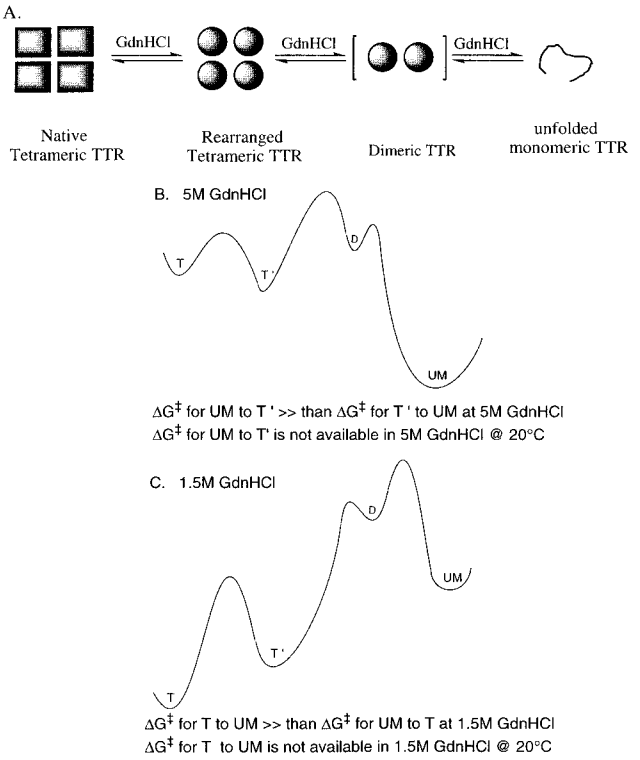

FIGURE 9: (A) Summary of GdnHCl denaturation pathway of wild-type TTR. Double-headed arrows do not imply that all of these equilibia are thermodynamically reversible; instead they mean that the forward and reverse reactions can both proceed, but not necessarily under the same conditions. (B) Free energy coordinate diagram consistent with the behavior of TTR under denaturing conditions at 5 M GdnHCl. The $\Delta G^{\ddagger}$ for denaturation of the rearranged TTR tetramer (T′) to the unfolded monomer (UM) is available, whereas the free energy of activation for the reverse reaction is not available; hence the UM and T′ are not in equilibrium in 5 M GdnHCl. (C) Free energy coordinate diagram consistent with the behavior of TTR undergoing reconstitution at 1.5 M GdnHCl. Upon dilution of denatured TTR (7 M GdnHCl) to 1.5 M GdnHCl, the $\Delta G^{\ddagger}$ for proceeding from unfolded monomer (UM) to tetramer (T) is available, whereas the free energy of activation for the reverse reaction is not available; hence the UM and T are not in equilibrium in 1.5 M GdnHCl.

below 2 M GdnHCl, indicating that nativelike β-sheet tertiary structure in TTR forms at concentrations below 2 M GdnHCl.

From the data presented above, it is clear that GdnHCl reconstitution and denaturation of TTR is not a simple two-state transition, even though tetramer and monomer comprise the vast majority of the quaternary species present at a given GdnHCl concentration. The conditions that achieve the denaturation and refolding transitions are separated by a concentration difference of approximately 4 M GdnHCl. Depending on the starting point, the kinetically accessible states at a given GdnHCl concentration differ. We propose the pathway for TTR denaturation in GdnHCl shown in Figure 9A, which is similar to the pathway elucidated by our group for acid denaturation of TTR (Lai et al., 1996). Under denaturing conditions, TTR exists as a tetramer over a GdnHCl concentration range of 0−4 M, possibly having a rearranged C-strand−loop−D-strand region at the higher end of this denaturant concentration range. Tetrameric TTR having a defined tertiary structure dissociates to an unfolded monomer over a concentration range of 4−6 M GdnHCl. At GdnHCl concentrations > 6 M, TTR adopts a largely unfolded monomeric structure. The reconstitution (folding and association) from unfolded monomer (7 M GdnHCl) does not occur until the GdnHCl concentration is <2 M.

Although double-headed arrows are used in the proposed pathway outlined in Figure 9A, this does not imply that this process is thermodynamically reversible but rather shows that the forward and reverse reactions can proceed, but not under the same conditions.

The observed hysteresis appears to result from a free energy coordinate that changes with GdnHCl concentration coupled to a situation where there is a significant kinetic barrier intervening between the folded tetramer and the unfolded monomer in both the denaturation and the reconstitution directions. The representative free energy reaction coordinates shown in Figure 9B,C, although likely oversimplified, rationalize the basis of the hysteresis observed. During denaturation in 5 M GdnHCl, for example, the $\Delta G^{\ddagger}$ for the T′ to UM pathway is available whereas the $\Delta G^{\ddagger}$ for the UM to T′ pathway is not; hence the back rate is essentially zero (Figure 9B). During reconstitution, dilution to 1.5 M GdnHCl is required such that $\Delta G^{\ddagger}$ is available for the UM to T′ transition; however, under these conditions $\Delta G^{\ddagger}$ for T′ to UM is not available (Figure 9C). A dimeric intermediate is pictured in Figure 9B,C because it is unlikely that tetrameric TTR dissociates directly to monomer or that monomer associates directly to tetramer, although at this time direct evidence does not exist to support the dimer intermediate.

In an effort to begin to better understand the details of the free energy coordinate diagrams, kinetic experiments were carried out under conditions where the TTR tetramer can dissociate to unfolded monomer but where the back reaction (unfolded monomer to tetramer) does not occur at a measurable rate. An estimate of the kinetic stability of TTR was obtained by measuring the rate constants for denaturation of the TTR tetramer over the GdnHCl concentration range of 6.2−7.4 M. Since the dissociation and unfolding appear to be linked, we followed unfolding of TTR by the disappearance of the β-sheet signal at 218 nm because the CD changes are not as complex as the changes in tryptophan fluorescence upon denaturation. Considering the mechanism presented in Figure 9A, the rearranged tetramer likely dissociates to dimeric TTR, which appears to be an unstable species and rapidly converts to unfolded monomer. Since we are following the CD signature for rearranged tetrameric TTR (nativelike far-UV CD signal) going to unfolded monomeric TTR, the rate constant measured is probably the unimolecular dissociation of rearranged TTR tetramer to dimeric TTR, which is the likely rate-determining step in the rearranged tetramer to unfolded monomer transition. This logic is consistent with the fact that the dimeric TTR never builds up in concentration. The rate data measured fit nicely to a single-exponential decay. The rate constants determined over a GdnHCl range of 6.2−7.4 M extrapolated to 0 M GdnHCl give a $k = (9.0 \pm 7.5) \times 10^{-11}$ s^{-1} for the unfolding of TTR tetramer under these conditions, which corresponds to a half-life of approximately 293 years. This demonstrates that the dissociation of TTR tetramer is indeed a very slow process and that the TTR tetramer and monomer are likely separated by a very high activation barrier.

The underlying assumption in the extrapolation above is that the rate-determining step in GdnHCl is the same as the step that characterizes dissociation and unfolding of TTR under conditions not involving denaturants, such as under physiological conditions. In their studies on T4 lysozyme, Chen and co-workers pointed out that this assumption is not always valid (Chen et al., 1992). Hence it is important to consider the possibility that the kinetic pathway could change in the absence of denaturing agents (Chen et al., 1992). Assuming the rate constant we obtained by extrapolation to 0 M GdnHCl represents the kinetic constant in the absence of GdnHCl, we can compare the kinetic stability of wild-type TTR to the stability exhibited by the FAP mutations associated with early onset amyloid disease. This is important because TTR is constantly turned over *in vivo* with a half-life of 1.5−2.5 days (Divino & Schussler, 1990; Makover et al., 1988); hence, the kinetic accessibility to the amyloidogenic conformation under denaturing conditions is probably as important as the thermodynamics of the denaturation process. An identical kinetic evaluation of the GdnHCl denaturation of Val-30-Met and Leu-55-Pro TTR, which are the most prevalent and most deleterious FAP-associated variants, respectively, yields an extrapolated rate constant on the order of 10^{-8} s^{-1} for each, corresponding to a half-life of several hundred days under physiological conditions! The Val-30-Met and Leu-55-Pro variants dissociate at least 3 orders of magnitude faster than wild-type TTR, which has a half-life of approximately 293 years. These results support our proposal that most of the FAP mutants do not act by altering the native structure of TTR (Kelly, 1996; Kelly & Lansbury, 1994; McCutchen et al., 1993, 1995); instead, these FAP mutations appear to alter the denaturation pathway by making either the thermodynamics or the kinetics or both favorable for formation of the amyloidogenic intermediate, which self-assembles into amyloid fibrils. A more detailed evaluation of denaturation kinetics of the FAP variants relative to that of the wild-type TTR is underway, under acidic conditions which yield the amyloidogenic intermediate.

For many small proteins, the native state is in equilibrium with the unfolded state in chaotropic solutions, implying that the kinetic barriers between the folded and unfolded states are readily surmountable (Dill, 1993). In this scenario, the position of the equilibrium is independent of the starting conditions and governed by the relative energies of the folded and unfolded states. On the other hand, if the quaternary and tertiary structure of a protein at a given chaotrope concentration depends on the initial conditions, at least one significant kinetic barrier exists somewhere on the pathway. This behavior has now been observed for several proteins (Baker & Agard, 1994; Baker et al., 1992; Mottonen et al., 1992; Gething et al., 1986; Eder et al., 1993; Banzon & Kelly, 1992; Jaenicke; 1995). Bacterial luciferase exhibits a hysteresis that is very similar to that exhibited by transthyretin in this study (Sinclair et al., 1994). The folding of β_2 dimer of luciferase is remarkably similar to that of TTR; namely, the β_2 dimer does not denature until 6 M urea, yet once denatured in 10 M urea, the β subunit remains unfolded until the urea concentration is $\leq$2 M. Clearly the free energy landscape for the denaturation and reconstitution of TTR and β_2 dimer of luciferase is rugged, and because of the high energy barriers, starting at different locations leads to different tertiary and quaternary structures at a given denaturant concentration (Chan & Dill, 1993). Mutation-induced changes in the free energy landscape governing TTR denaturation may play a role in human amyloid disease by making partial denaturation more facile, such as in the case of the Val-30-Met mutation that is associated with FAP. The generality of activation barrier lowering by the FAP muta-

tions and the relevance of GdnHCl denaturation to denaturation *in vivo* will receive further scrutiny.

REFERENCES

Baker, D., & Agard, D. A. (1994) *Biochemistry 33*, 7505−7509.
Baker, D., Sohl, J. L., & Agard, D. A. (1992) *Nature 356*, 263−265.
Banzon, J. A., & Kelly, J. W. (1992) *Protein Eng. 5*, 113−115.
Benson, M. D. (1989) *Trends Biochem. Sci 12*, 88−92.
Benson, M. D., & Wallace, M. R. (1989) in *The Metabolic Basis of Inherited Disease*, pp 2439−2460, McGraw-Hill, NY.
Blake, C., & Serpell, L. (1996) *Structure 4*, 989−998.
Blake, C. C. F., Geisow, M. J., Swan, I. D. A., Rerat, C., & Rerat, B. (1974) *J. Mol. Biol. 88*, 1−12.
Blake, C. C. F., Geisow, M. J., & Oatley, S. J. (1978) *J. Mol. Biol. 121*, 339−356.
Branch, W. T., Robbins, J., & Edelhoch, H. (1972) *Arch. Biochem. Biophys. 152*, 144−151.
Caughey, B. W., Dong, A., Bhat, K. S., Ernst, D., Hayes, S. F., & Caughey, W. S. (1991) *Biochemistry 30*, 7672−7680.
Chan, H. S., & Dill, K. A. (1993) *J. Chem. Phys. 99*, 2116−2127.
Chen, B., Baase, W. A., Nicholson, H., & Schellman, J. A. (1992) *Biochemistry 31*, 1464−1476.
Cohen, A. S., Shirahama, T., Sipe, J. D., & Skinner, M. (1983) *Lab. Invest.* 48, 1−4.
Colon, W., & Kelly, J. W. (1991) in *Applications of Enzyme Biotechnology* (Kelly, J. W., & Baldwin, T. O., Eds.) Plenum, pp 99−108, New York.
Colon, W., & Kelly, J. W. (1992) *Biochemistry 31*, 8654−8660.
Come, J. H., & Lansbury, P. T., Jr. (1994) *J. Am. Chem. Soc. 116*, 4109−4110.
Cornwell, G. G., Sletten, K., Johansson, B., Westermark, P. (1988) *Biochem. Biophys. Res. Commun. 154*, 648−653.
Dill, K. A. (1993) *Curr. Opin. Struct. Biol. 3*, 99−103.
Dill, K. A., & Shortle, D. (1991) *Annu. Rev. Biochem. 60*, 795−825.
Divino, C. M., & Schussler, G. C. (1990) *J. Biol. Chem. 265*, 1425−1429.
Durchschlag, H., & Jaenicke, R. (1982) *Biochem. Biophys. Res. Commun. 108*, 1074−1079.
Durchschlag, H. (1986) in *Thermodynamic Data for Biochemistry and Biotechnology* (Hinz, H.-J., Ed.) Chapt. 3, p 45, Springer-Verlag, New York.
Durchschlag, H., & Jaenicke, R. (1983) *Int. J. Biol. Macromol. 5*, 143−148.
Eder, J., Rheinnecker, M., & Fersht, A. R. (1993) *Biochemistry 32*, 18−26.
Eftink, M. R. (1994) *Biophys. J. 66*, 482−501.
Fraser, P. E., McLachlan, D. R., Surewicz, W. K., Mizzen, C. A., Snow, A. D., Nguyen, J. T., & Kirschner, D. A. (1994) *J. Mol. Biol. 244*, 64−73.
Furuya, H., Saraiva, M. J. M., Gawinowicz, M. A., Alves, I. L., Costa, P. P., Sasaki, H., Goto, I., & Sakaki, Y. (1991) *Biochemistry 30*, 2415−2421.
Gething, M.-J., McCammon, K., & Sambrook, J. (1986) *Cell 46*, 939−950.
Glenner, G. G., Ein, D., Eanes, E. D., Bladen, H. A., Terry, W., & Page, D. L. (1971) *Science 174*, 712−714.
Gustavsson, Å., Engstrom, U., & Westermark, P. (1991) *Biochem. Biophys. Res. Commun. 175*, 1159−1164.
Hamilton, J. A., Steinrauf, L. K., Braden, B. C., Liepnieks, J., Benson, M. D., Holmgren, G., Sandgren, O., & Steen, L. (1993) *J. Biol. Chem. 268*, 2416−2424.
Hurle, M. R., Helms, L. R., Li, L., Chan, W., & Wetzel, R. (1994) *Proc. Natl. Acad. Sci. U.S.A. 91*, 5446−5450.
Jacobson, D. R., & Buxbaum, J. N. (1991) *Adv. Hum. Genet. 20*, 69−123.
Jaenicke, R. (1995) *Philos. Trans. R. Soc. London, Ser. B: Biol. Sci. 348*, 97−105.
Kelly, J. W. (1996) *Curr. Opin. Struct. Biol. 6*, 11−17.
Kelly, J. W., & Lansbury, P. T. J. (1994) *Amyloid: Int. J. Exp. Clin. Invest. 1*, 186−205.
Lai, Z., Colon, W., & Kelly, J. W. (1996) *Biochemistry 35*, 6470−6482.
Lai, Z., Lashuel, H. A., & Kelly, J. W. (1997) *Biochemistry* (submitted for publication).
Lakowicz, J. R. (1983) *Principles of Fluorescence Spectroscopy*, Plenum Press, New York.
Laue, T. (1992) in *Analytical Ultracentrifugation in Biochemistry and Polymer Science*, pp 90−125, Redwood Press Ltd., Cambridge, England.
Lee, J. C., & Timasheff, S. N. (1979) *Methods Enzymol. 61*, 49−59.
Lee, J. P., Stimson, E. R., Ghilardi, J. R., Mantyh, P. W., Lu, Y. A., Felix, A. M., Llanoss, W., Behbin, A., Cummins, M., Vancriekinge, M., Timms, W., & Maggio, J. E. (1995) *Biochemistry 34*, 5191−5200.
Makover, A., Moriwaki, H., Ramakrishnan, R., Saraiva, M. J. M., Blaner, W. S., & Goodman, D. S. (1988) *J. Biol. Chem. 263*, 8598−8603.
Miroy, G. J., Lai, Z., Lashuel, H. A., Peterson, S. A., Strang, C., & Kelly, J. W. (1996) *Proc. Natl. Acad. Sci. U.S.A. 93*, 15051−15056.
McCutchen, S., Colon, W., & Kelly, J. W. (1993) *Biochemistry 32*, 12119−12127.
McCutchen, S. L., Lai, Z., Miroy, G., Kelly, J. W., & Colon, W. (1995) *Biochemistry 34*, 13527−13532.
McMeekin, T. L., & Marshall, K. (1952) *Science 116*, 142−145.
Mottonen, J., Strand, A., Symersky, J., Sweet, R. M., Danley, D. E., Geoghegan, K. F., Gerard, R. D., & Goldsmith, E. J. (1992) *Nature 355*, 270−273.
Pace, C. N. (1975) *Crit. Rev. Biochem. 3*, 1−43.
Pace, C. N., Shirley, B. A., & Thormson, J. A. (1989) in *Protein Structure: A Practical Approach*, pp 311−330, IRL Press, New York.
Pepys, M. B., Hawkins, P. N., Booth, D. R., Vigushin, D. M., Tennent, G. A., Soutar, A. K., Totty, N., Nguyen, O., Blake, C. C. F., Terry, C. J., et al. (1993) *Nature 362*, 553−557.
Perkins, S. J. (1986) *Eur. J. Biochem. 157*, 169.
Philo, J. S. (1994) in *Modern Analytical Ultracentrifugation*, pp 156−170, Birkhauser, Boston, MA.
Prusiner, S. B. (1991) *Science 252*, 1515−1522.
Saraiva, M. J. M. (1995) *Hum. Mutat. 5*, 191−196.
Saraiva, M. J. M., Costa, P. P., & Goodman, D. S. (1983) *J. Lab. Clin. Med. 102*, 590−603.
Saravia, M. J. M., Birken, S., Costa, P., & Goodman, D. S. (1984) *J. Clin Invest. 74*, 104−119.
Saraiva, M. J. M., Costa, P. P., & Goodman, D. S. (1988) *Adv. Neurol. 48*, 189−200.
Shortle, D., Meeker, A. K., & Gerring, S. L. (1989) *Arch. Biochem. Biophys. 272*, 103−113.
Sinclair, J. F., Ziegler, M. M., & Baldwin, T. O. (1994) *Nat. Struct. Biol. 1*, 320−326.
Stafford, W. F. (1994) *Methods Enzymol. 240*, 478−501.
Steinrauf, L. K., Hamilton, J. A., Braden, B. C., Murrell, J. R., & Benson, M. D. (1993) *J. Biol. Chem. 268*, 2425−2430.
Stone, M. J. (1990) *Blood 75*, 531−545.
Terry, C. J., Damas, A. M., Oliveira, P., Saraiva, M. J., Alves, I. L., Costa, P. P., Matias, P. M., Sakaki, Y., & Blake, C. C. F. (1993) *EMBO J. 12*, 735−741.
Thomas, P. J., Qu, B.-H., & Pedersen, P. L. (1995) *Trends Biochem. Sci. 20*, 456−459.
Westermark, P., Sletten, K., Johannson, B., & Cornwell, G. G. (1990) *Proc. Natl. Acad. Sci. U.S.A. 87*, 2843−2845.

BI963195P